

Robust estimation of spectral reflectance by a projector-camera system

Yuqi Li (李裕麒)^{1*}, Dongming Lu (鲁东明)¹, and Lei Zhao (赵磊)¹

College of Computer Science and Technology, Zhejiang University, Hangzhou 310027, China

*Corresponding author: fenghuoqilin@gmail.com

Received July 11, 2013; accepted September 16, 2013; posted online November 4, 2013

A Projector-camera (Procam) system is an inexpensive, household, controllable system that can be used to eliminate inter-reflection existing in the measurement. We propose an estimation method for spectral reflectance that uses the Procam system. The method recovers reflectance from the training set constructed by a known reflectance and the corresponding 9D color-mixing matrix. Experiment results show that our method performs well with 9D response, and the local weighted training set based on Mahalanobis metric can enhance the accuracy of result efficiently.

OCIS codes: 330.1690, 330.7310.

doi: 10.3788/COL201311.113301.

Estimating the spectral reflectance of objects or scenes in visible wavelengths is useful in numerous vision tasks such as material recognition, relighting, multispectral projection display, etc. Although using a spectrophotometer and the illumination sequences of specific wavelengths is a precise way to recover spectral reflectance, it is not practical since the laboratory instruments are expensive and require professional training. Hence, methods that use multi-spectral imaging systems have been proposed as a substitute to using spectrophotometers^[1–4]. These methods can estimate the spectral reflectance from the training samples without known a illumination spectrum and spectral sensitivity. The training samples are constructed with abundant spectral reflectance and the corresponding camera response. However, these multi-spectral imaging techniques cannot deal with concave objects in the presence of inter-reflection because inter-reflection that exists in the measurement may cause inaccurate results.

Benefit from encoded patterns techniques^[5] of the Projector-camera (Procam) system, we can separate direct and indirect light rapidly which cannot be realized with other controllable light sources. The system that combines controllable projectors with cameras is popular in a wide range of applications, such as three-dimensional (3D) scanning, flexible display walls^[6], light field acquisition, and interaction. Han *et al.*^[7] used a digital light processing (DLP) projector and a camera to recover reflectance, but the method requires the spectral sensitivity of camera to be known. As mentioned above, the method is inaccurate and the process may cause accumulated errors without laboratory measurements. Furthermore, previous prior-free methods^[1–4] are also impractical for estimation reflectance using the Procam system since the adjacent channels of the Procam system are highly correlated. These methods are not applicable to high correlation datasets. In this letter, a robust prior-free method is proposed. We will show the local weighted samples based on Mahalanobis metric are more appropriate for estimating spectral reflectance by using the Procam system.

The method is largely inspired by the Procam color-

mixing (PCCM) matrix which was introduced to radiometric compensation previously^[8]. The 3×3 matrix is defined to describe the behavior of projection surface in the feedback of a Procam system. Spectral reflectance is an intrinsic characteristic independent of the spectral distribution of illumination and sensitivity of camera sensors, thus we estimate it from the PCCM matrix. By using a known spectral reflectance and the corresponding PCCM matrix of the training samples, the goal spectral reflectance can be recovered. To recover the absolute reflectance ratio each time, a certain distance between the projector and the reflection surface is necessary. Obviously, we can solve the extrinsic parameters (pose and position) of a Procam system by using geometric calibration techniques^[9]. In practice, we use a 24 color-Macbeth chart to create the training set. The PCCM matrix of several color chips on the Macbeth chart is shown in Fig. 1.

In general, the response model based on the Procam system can be expressed as

$$C_{mn} = \int (P_m l_m(\lambda) + e(\lambda)) s_n(\lambda) r(\lambda) d\lambda, \quad (1)$$

where C_{mn} is the response of n th channel under the m th illumination, $e(\lambda)$ is the spectral distribution of noise light, $l_m(\lambda)$ is the spectral distribution of the m th projector channel, $r(\lambda)$ is the spectral reflectance of a surface

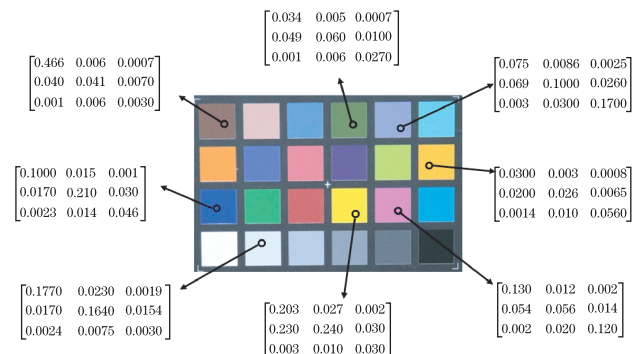


Fig. 1. PCCM matrix of the color chips on the Macbeth chart.

point, P_m is the radiant intensity of each channel and $s_n(\lambda)$ is the spectral sensitivity of the n th camera channel. The noise consists of ambient light and the black offset of projector, it can be cancelled by subtracting another captured image with changing the illumination in one channel as follows:

$$\Delta C_n = \sum_{m=1}^M P_m \int l_m(\lambda) s_n(\lambda) r(\lambda) d\lambda. \quad (2)$$

In Fig. 2, we show the required four images to create the PCCM matrix for each pixels. Rewriting Eq.(2) into matrix form, we obtain

$$\begin{bmatrix} \Delta C_R \\ \Delta C_G \\ \Delta C_B \end{bmatrix} = \begin{bmatrix} V_{RR} & V_{RG} & V_{RB} \\ V_{GR} & V_{GG} & V_{GB} \\ V_{BR} & V_{BG} & V_{BB} \end{bmatrix} \times \begin{bmatrix} P_R \\ P_G \\ P_B \end{bmatrix}, \quad (3)$$

where V is the PCCM matrix. $l_m(\lambda)$ and $s_n(\lambda)$ are fixed in a Procam system, thus the element V_{mn} in the PCCM matrix is a constant that represents the average reflectance in the domain of $l_m(\lambda)s_n(\lambda)$. Referring to the database of spectral sensitivity functions measured by Jiang *et al.*^[10], wide domain intersections are found to exist between the spectral sensitivity $s_n(\lambda)$ of each channel. In addition, the sum of the three channels $\Sigma l_m(\lambda)$ generally covers entire visible wavelengths. The two factors of Procam system ensure that the elements in the PCCM matrix are larger than 0.

As mentioned above, it is convenient to eliminate ambient light error by subtracting a base image. In practise, however, inter-reflection among patches on measured objects may introduce significant errors, such errors can not be eliminated by using an uncontrollable light source. To separate direct and indirect light, we create four high-frequency color-coded multiplexing patterns as shown in Fig. 3.

The i th pattern P_c^i of channel c is modulated as

$$\begin{cases} P_c^i = \frac{1}{2} + \frac{1}{2} \sin\left(\frac{2\pi}{5} N_c i + \phi_c(x, y)\right) \\ C_c^i = \sum P_{c'}^i V_{c'c} + \frac{1}{2} L_c \quad (c, c' \in \{R, G, B\}) \end{cases}, \quad (4)$$

where N_c is the parameter of each channel to control modulation frequency, i is the sequence number of the

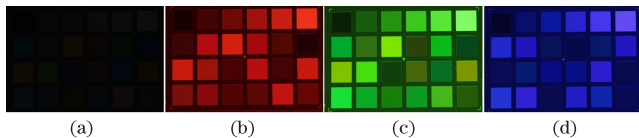


Fig. 2. Macbeth-color-chart images captured by a camera under different illumination of projector: (a) base illumination, (b) change red channel, (c) change green channel, and (d) change blue channel.



Fig. 3. Four high-frequency color-coded multiplexing patterns.

pattern and $\phi_c(x, y)$ is the phase of point (x, y) on the pattern image in the c channel, both N_c and $i \in \{1, \dots, 4\}$. C_c^i is the corresponding camera response of pattern P_c^i and L_c is the indirect light (inter-reflection) of the c channel. It worth notice that L_c is a constant since an assumption can be made that indirect component light remains constant as high-frequency patterns shift^[11]. Thus, after capturing the image with the maximum illumination (all channel are 1), we can obtain the maximum response \bar{C}_c , where $\bar{C}_c = \sum V_{c'c} + L_c (c' \in \{R, G, B\})$. Indirect light L_c can be removed as

$$C_c^i = \frac{1}{2} \left(\bar{C}_c + \sum \sin\left(\frac{2\pi}{5} N_c i + \phi_c(x, y)\right) V_{c'c} \right) \quad (c, c' \in \{R, G, B\}). \quad (5)$$

Three unknown variables $\phi_c(x, y)$ and nine $V_{c'c}$ exist in the equations, thus, we have twelve unknown variables. $3 (\text{channels}) \times 4 (\text{patterns}) = 12$ equations is sufficient to derive the direct-reflection solution.

The spectral distribution of an liquid crystal display (LCD) projector and the spectral sensitivity of a digital camera measured by a spectrophotometer are shown in Fig. 4(a) and (b), respectively. In this letter, we apply the training set (\mathbf{X}, \mathbf{R}) to determine the spectral reflectance, where \mathbf{X} is the set of 9D PCCM vectors $\mathbf{x} = [V_{RR}, V_{RG}, V_{RB}, V_{GR}, V_{GG}, V_{GB}, V_{BR}, V_{BG}, V_{BB}]$ and \mathbf{R} is the set of the corresponding spectral reflectance. In general, subspace dimension of real-world materials reflectance is 5-8^[12]; therefore, the vector is applicable and sufficient to recover natural reflectance. Furthermore, we can use inexpensive wide-band filters to increase the number of channels and reduce the possible effects of metamerism.

The linear pseudo-inverse method is a simple and robust tool for estimating spectral reflectance without any prior knowledge. Given a input vector \mathbf{x} and a training set (\mathbf{X}, \mathbf{R}) , we can estimate the reflectance r using the normal equations as follows:

$$\mathbf{r} = \mathbf{R}\mathbf{X}(\mathbf{X}^T\mathbf{X})^{-1}\mathbf{x}. \quad (6)$$

It is worth notice that training samples neighbors are usually more reliable and contribute more to the estimation. Therefore, instead of global inversion and regression method, we use a local definition to provide more accurate results^[13]. That is, an spectral reflectance r can be reconstructed by k nearest neighbors. It is reasonable since a sample in high dimension can be represented as a linear combination of its neighborhood according to the theory of local manifold embedding. Thus the key issue becomes how to select k appropriate neighborhoods from the training set.

Unlike reflectance estimation from the response of trichromatic camera or multi-spectral narrow-band camera, higher correlations exist among variables in the vector as shown in Fig. 4 (c), particularly between adjacent channels. Moreover, due to the significant difference (almost two orders of magnitude) among measure vectors $l_m(\lambda)s_n(\lambda)$, neighborhoods selection should also account for scaling each coordinate axis. In our method, neighborhoods will be selected according to the Mahalanobis distance rather than the Euclidean distance. We define the distance between vectors x and x_i as

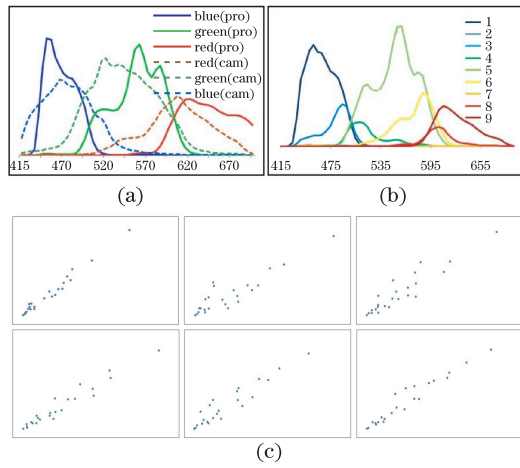


Fig. 4. (a) Spectral distribution of a projector and spectral sensitivity of a camera, (b) spectral distribution of Procama nine channels, and (c) distribution of adjacent channels of the PCCM vector on Macbeth chart (from first to last: $V_{RR} - V_{RG}$, $V_{RG} - V_{BR}$, $V_{BR} - V_{BB}$, $V_{BB} - V_{BG}$, $V_{BG} - V_{GG}$, $V_{GG} - V_{GB}$).

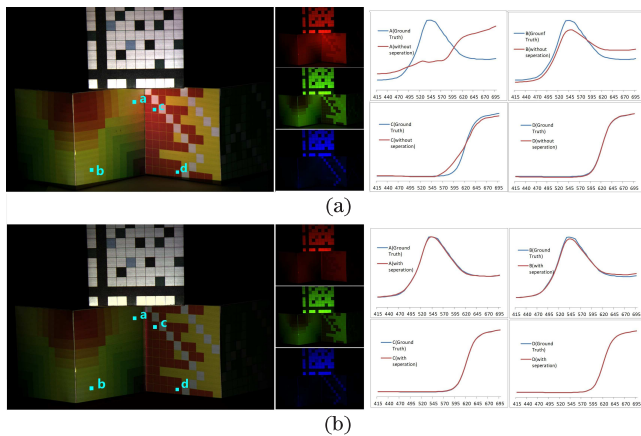


Fig. 5. (Color online) Spectral reflectance recovery (a) without inter-reflection removal and (b) with inter-reflection removal. The estimated reflectance spectra of regions a, b, c, d are shown as solid lines (red: estimated reflectance in the concave scene as shown in the images, green: estimated reflectance in a uniform illumination scene (not appearing in the images)). The materials of regions a and b, c and d are the same (zoom in to see details).

$$D(x, x_i) = (\sqrt{x - x_i})^T \mathbf{S}^{-1} (x - x_i), \quad (7)$$

where \mathbf{S} is the covariance matrix of samples. It is worth notice that the performance of the Mahalanobis distance is not stable because of its dependence on training samples. We should ensure that the size of training set is larger than the number of channels ($k > 9$) and remove the linearly independent samples, or using the standard Euclidean distance once the Mahalanobis distance becomes invalid.

Although the neighbor samples $\{\cup x_i | i = 1, \dots, k\}$ are reliable to estimate reflectance from the candidate x , the contribution of each sample x_i should not be equal since the distance $D(x, x_i)$ are different. Motivated by the optimized adaptive estimation method proposed by Shen *et al.*^[14], we construct the training set $(\tilde{\mathbf{X}}, \tilde{\mathbf{R}})$ with weighted neighbor samples $\{(\alpha_i x_i, \alpha_i r_i) | i = 1, \dots, k\}$ in

this letter. The weighted α_i is

$$\alpha_i = \exp \left[-\frac{1}{2} (x - x_i)^T \mathbf{S}_k^{-1} (x - x_i) \right], \quad (8)$$

where \mathbf{S}_k^{-1} is the covariance matrix of k neighbor samples. Then, the reflectance r can be solved as

$$r = \tilde{\mathbf{R}} \tilde{\mathbf{X}} (\tilde{\mathbf{X}}^T \tilde{\mathbf{X}})^{-1} x, \quad (9)$$

where $(\tilde{\mathbf{X}}, \tilde{\mathbf{R}})$ is the local weighted training set.

In the first experiment, we test our inter-reflection removal (separation) and the reflectance estimation method in a concave scene that consists of three color chip boxes. As shown in Fig. 5 (a), there is a significant inter-reflection exists between two surfaces of the bottom boxes. The inter-reflection causes redundant illumination and color deviation, which result in inaccurate camera response.

We use an LCD projector (EPSON EB300MS), a camera (Canon 5D MarkII) and training samples of Macbeth CDC 24 chips color-check to recover the reflectance of regions a, b, c, d with and without inter-reflection removal. We also recover the reflectance in an uniform illumination scene without any inter-reflection for comparison purposes. As shown in Fig. 5, the estimated value with inter-reflection removal (bottom) matches the ground truth better than value with inter-reflection removal (up), particularly in region a and b. The results show that our inter-reflection removal method with a Procama system is efficient and robust.

In the second experiment, we compare our local weighted pseudo-inverse method with the optimized adaptive estimation method and the global pseudo-inverse method by simulating with large amounts of samples as shown in Table 1. Projector illumination and camera responses are simulated based on the actual spectral distribution of a projector and actual spectral sensitivity of a camera. In this case, to meet to ordinary situation, we add random Gaussian white noise \mathbf{e} to camera response \mathbf{x} ($\frac{\|\mathbf{e}\|}{\|\mathbf{x}\|} = 0.004$).

Table 2 shows the reflectance errors of the three methods on the validation sets with samples sizes $N = 100, 200, 300, 600$ randomly selected from the training set. By comparing the average and maximum root-mean-square error (RMSE) of each method, we observe that our method shows the best performance. Benefiting from the weighted training set, the optimized adaptive estimation method and our method perform better than the global pseudo-inverse method. Moreover, the neighbor training set with the appropriate size k makes the results of our method better than the results of the optimized adaptive estimation method. The best results in Table 2 are provided by setting $K = 40, 80, 180, 280$. Therefore, we can draw a conclusion that the best k is dependent on the size of the original training set ($K \approx \frac{N}{2}$).

Table 1. Datasets for the Experiment^[15].

Dataset	Name	Size
Training Set	Munsell Matte	100, 200, 300, 600
Validation Set	Natural Colors	219
Testing Set	Agfa IT8.7/2	288
	Macbeth CDC	24

Table 2. Estimation Errors on the Testing Set

Training Size		Our Method	Optimized AE	Pseudo-inverse
100	Mean	0.1360	0.1372	0.1957
	Max	0.2063	0.2490	0.6408
200	Mean	0.1333	0.1372	0.1902
	Max	0.2062	0.2696	0.6269
300	Mean	0.1261	0.1311	0.1874
	Max	0.2789	0.2915	0.6101
600	Mean	0.1180	0.1262	0.1742
	Max	0.2141	0.2385	0.6052

In conclusion, we propose an estimation method for spectral reflectance using a Procams system. The method eliminates inter-reflection and makes more accurate measurement. Making use of the color-mixing matrix, our method can recover reflectance from training without prior knowledge of the spectral distribution of the illumination and the spectral sensitivity of the camera. We introduce an inter-reflection removal method to produce a more accurate camera response. In addition, we adopt the Mahalanobis metric and local weighted training samples to eliminate the effect of data correlation and to enhance accuracy.

This work was supported by the National Basic Research Program of China (No. 2012CB725305) and the National Natural Science Foundation of China (No. 61003146). We thank the reviewers for their helpful suggestions.

References

- J. I. Park, M. H. Lee, M. D. Grossberg, and S. K. Nayar, in *Proceedings of the IEEE International Conference on Computer Vision* 1 (2007).
- W. Zhang, G. Tang, D. Dai, and A. Nehorai, *Opt. Lett.* **36**, 3933 (2011).
- V. Heikkinen, T. Jetsu, J. Parkkinen, M. Hauta-Kasari, T. Jaaskelainen, and S. D. Lee, *J. Opt. Soc. Am. A* **24**, 2673 (2007).
- W. Zhang and D. Dai, *J. Opt. Soc. Am. A* **25**, 2286 (2008).
- D. Reddy, R. Ramamoorthi, and B. Curless, *Lecture Notes in Computer Science* **7577**, 596 (2012).
- L. Qi, Q. Wang, J. Lup, A. Wang, and D. Liang, *Chin. Opt. Lett.* **10**, 011101 (2012).
- S. Hzn, I. Sato, T. Okabe, and Y. Sato, *Lecture Notes in Computer Science* **6492**, 323 (2011).
- M. D. Grossberg, H. Peri, S. K. Nayar, and P. N. Belhumeur, in *Proceedings of the IEEE Computer Society Conference on Computer Vision and Pattern Recognition* 452 (2004)
- B. Sajadi and A. Majumder, *Computer Graphics Forum* **29**, 1063 (2010).
- J. Jiang, D. Liu, J. Gu, and S. Susstrunk, in *Proceedings of IEEE Workshop on Applications of Computer Vision* 168 (2013)
- J. Gu, T. Kobayashi, M. Gupta, and S. K. Nayar, in *Proceedings of the IEEE International Conference on Computer Vision* 691 (2011)
- J. P. Parkkinen, J. Hallikainen, and T. Jaaskelainen, *J. Opt. Soc. Am. A* **6**, 318 (1989).
- H. Ville, L. Reiner, J. Tuija, P. Jussi, H.-K. Markku, and J. Timo, *J. Opt. Soc. Am. A* **25**, 2444 (2008).
- H. -L. Shen and J. H. Xin, *J. Opt. Soc. Am. A* **23**, 1566 (2006).
- “Spectral database”, <http://www.uef.fi/spectral/spectral-database>.